# A Stochastic Model of the Effector T Cell Lifecycle

John Burns[1,2] and Heather J. Ruskin[1]

[1] School of Computing, Dublin City University, Dublin 9, Ireland
[2] Department of Computing, Institute of Technology Tallaght, Dublin 24, Ireland
jburns@computing.dcu.ie

**Abstract.** The dynamics of immune response to initial infection and reinfection by the same pathogen sometime later, are considerably different. Primary response, which follows initial infection, is characterised by relatively slow precursor cell activation and population growth rates, with a consequent elongated pathogen clearance profile, typically extended over six days or more. On the other hand, secondary response (to reinfection by the same pathogen some time later) is notable for short effector activation time, high specificity of response, rapid pathogen elimination and high degree of memory cell participation. In this paper, we present a seven state non-deterministic finite automata (NFA) of the effector T cell lifecycle, which is encoded as a set of states and state transitions. Our objective is to study the degree to which variable infection outcome is dependent on the accumulation of *chance* events. Such chance events may be represented as the consequence of premature, delayed or even failed state transitions. We show how small variation in crucial state transitions probabilities during the lifecycle can induce widely variable infection outcomes. This model is implemented as a spatially extended, concurrent two-dimensional stochastic cellular automata, executing on a MPI-based Linux cluster.

## 1 Introduction

Cellular Automata (CA) have been applied to numerous areas of complex physical systems modelling [1]. CA have several important characteristics which make them amenable to efficient computational implementation, including ease of representing (in the form of $n$-dimensional arrays), discrete nature of the underlying computations, simplicity of rules or laws which are programmed into the CA, and the highly repetitious nature of the processing steps. However, cellular automata posses additional fascinating properties, for example, patterns of self-organisation of a complexity which cannot be derived numerically from the rules on which the underling cellular automata is based. As a result of this complexity, [2] has postulated that some form of CA must underlie many complex physical phenomena visible in nature. Furthermore, with the application of non-deterministic (*stochastic*) cellular automata, the idea of randomness in CA site

P.M.A. Sloot, B. Chopard, and A.G. Hoekstra (Eds.): ACRI 2004, LNCS 3305, pp. 454–463, 2004.

selection and update rule enforcement has yielded further insight into modelling stochastic natural systems such as molecular motion, turbulence in water flow and various biological processes, especially models of the human immune system [3,4,5,6,7]. In this paper we present an approach that seeks to avoid a computational modelling process exclusively influenced by current experimental immune system research trends. We propose a *relaxation* of the deterministic assumptions inherent in earlier work [8], and explore the dynamics of a more stochastic system. Stochastic events appear to play a crucial role in certain immune system functions [9]. The contribution of this work is as follows: (i) an extended non-deterministic state transition model of the effector T cell lifecycle is introduced. This model successfully reproduces time-realistic effector and pathogen population dynamics during primary and secondary response, and during repeated reinfection, (ii) we identify three stages in the effector T cell lifecycle model which are critical in regulating the course of primary and secondary response, and (iii) the model is implemented as a spatially extended two-dimensional cellular automata lattice executing concurrently on a MPI-based Linux cluster. This allows us to scale the model to cell density levels in the order of $10^6$ CTL cells - which approaches levels typically observed in *in-vivo* murine experiments. This work is arranged as follows: section 2 is a brief overview of some key features of the adaptive immune response which we model, and serves as an introduction to some specific terminology. Section 2 is intended for readers who may be unfamiliar with general principles of immunology. Section 3 discusses the model structure and explains the motivation and implementation of the underlying non-deterministic cellular automata. Section 4 presents results of the simulation, and in particular, some interesting features which emerge. Finally, section 5 is a discussion of the results, and an outline of further enhancements.

## 2 Adaptive Immune Response

Common to all immune systems is the principal of sensing of localised space for the purposes of intrusion detection. Intrusion, in this case, is the appearance of a bacteria, viral particle or infected cell which may be classified as *non-self*. Any non-self genetic material discovered must be eliminated in order to prevent infection (or even death), of the host. Broadly speaking, the means by which the non-self intruder gained access to the blood stream or lymphatic compartments is not of interest[1]. There are a great variety in the pathogen challenge and immune response course (not all of which are a concern here). One such scenario arises as follows: when a viral particle has been taken up by an antigen-presenting cell (APC), such as a dendritic cell, it is degraded into one or more peptide chains within the cytosol region of the APC, and is then bound to the major histocompatible complex (MHC) class I molecule (a process known as *antigen processing*) before finally being presented on the surface of the APC as

[1] Some viruses, for example, the influenza and corona viruses, enter the host through the air passages and not through tissue damage.

an MHC:peptide complex, a process known as *antigen presenting*. APC will recirculate through the lymphatic system in order to alert the immune system to an infection. Sensing of the lymphatic compartments (of which there are many) for antigen-presenting cells, is a systematic function of immune cell (lymphocyte) recirculation. Cytotoxic lymphocyte (CTL) precursor cells constantly recirculate and sample their environment in the search for foreign pathogens. The process of sampling involves two cells binding for some small time period, during which the immune cell senses the receptor of the bound cell to determine if the bound cell is an invading pathogen (or not). If the bound cell *is* an invading pathogen, the immune cell may be stimulated to produce clones of itself in order to attack and remove other cells bearing the same genetic material. Under normal circumstances, the production of clones ceases after some fixed period of time, and once the infection has been cleared, most CTL cells will undergo programmed death (apoptosis). A small subset of the clone population will remain activated indefinitely, and this population represents effector memory. In the presented here, we do not model free antigen, but only antigen epitopes which have been bound to the surface of an antigen presenting cell.

## 3 The Model

Our model runs in discrete 30-minute timesteps, and all entities in the model act asynchronously at each timestep ($\tau$). As primary response normally consists of 4 days of cell replication (clonal expansion), the cells in our model will stop dividing at $\tau = 192$. The recirculation space of the lymphatic compartment is modelled as a two dimensional stochastic cellular automata lattice of length $L = 10^3$, with periodic boundary conditions and neighbourhood radius $r = 1$ (in two-dimensions), with a maximum of 8 neighbours. Each site is selected at random for update during the timestep. Not every site is will be visited at each timestep, but each site can be updated at most once in any given timestep. At $\tau = 0$ some 5000 antigen entities are introduced into randomly selected sites on the lattice (following a uniform distribution), and the model executes until $\tau = 3000$ (62.5 days of elapsed time). The CTL population grows exponentially in response to APC stimulation, with a clonal expansion rate which is a function of the *affinity* between the CTL and APC. The dynamics of affinity are modelled using shape space [10,11]. The stimulation rate never exceeding 0.036, which yields a population of daughter clones of $\sim 1000$ after 4.5 days of clonal expansion. Each lattice site may contain only one entity at any given timestep. The set of entities and states supported is shown in Table 1, which also introduces some important notation used throughout this paper.

### 3.1 Non-deterministic Finite Automata

To allow the study of a *distribution* of possible outcomes, we identify a subset of the CTL lifecycle state transitions, and replace the certainty of a transition from state $w$ to state $v$ on event $e$ with some probability ($< 1$) of state transition.

Let us start by defining what is meant by state transition relaxation: If $X$ is a discrete random variable ($drv$) representing the transition from state $w$ to state $v$, and $e$ is some event linking $wv$, the relaxed state transition $X_r$ is:

$$P(X_r|e) = 0 \leq \psi \leq 1 \tag{1}$$

The choice of value for $\psi$ will naturally depend on the $wv$ in question. In contrast to earlier models [2], Eq. (1) implies *duality* in the presence of event $e$: transition on $e$ ($X_r$) or not ($\bar{X}_r$). This extension results in a *non-deterministic* finite automaton (NFA) [12]. Fig. (1) is a non-deterministic finite automata model of the lifecycle of the CTL (and follows notation explained in Table 1). $E$ is the set of events the model, and consists of both deterministic and non-deterministic elements. We define a subset of three critical non-deterministic events $S \subset E$ as: $S = \{e_{2,8}, e_3, e_5\}$. Each $e_i \in S$ is defined as follows:

$e_2, e_8$ An infected antigen presenting cell will be destroyed by a bound cytotoxic lymphocyte cell which recognises it. Recognition is a function of the distance between the two cells in shape space.

$e_3$ An activated proliferating immune cell (state $ctl^{+\star}$) will normally end clonal expansion on the event $\langle e_3 : age(ctl^{+\star}) > 192\rangle$.

$e_6$ The fraction of effector T cells entering the long-lived memory pool. Normally the majority of activated effector cells undergo programmed cell death (apoptosis) at the end of primary response. However, recruitment to the memory pool consumes around $5 - 10\%$ of activated CTL [13,14, 15], thus, a further stochastic transition occurs on $e_6$, with of $ctl^{+\dagger}$ enter $ctl^{+\bullet}$ on event $\langle e_6 : age(ctl^{+\dagger}) \geq 192\rangle$.

$e_{rpt}$ Repeated reinfection events, resulting in repeated doses of infected antigen presenting cells introduced into the simulation, at timestep $\tau + 300n, n = 0, 1, ..., 9$.

Each of the above events ($e_n$) has an associated probability $\psi_n$. The set $\{\psi_1, \psi_2, \psi_3, \psi_4\}$, therefore fully describes each simulation configuration of the model (all other parameters being kept constant). In the results presented in the following section, we define the following four experimental onfigurations of $\mathcal{P}$:

1. $\mathcal{P}_1 : \{0.9, 0.9, 0.9, 0.0\}$
2. $\mathcal{P}_2 : \{0.9, 0.9, 0.95, 0.0\}$
3. $\mathcal{P}_3 : \{0.9, 0.9, 0.9, 1\}$
4. $\mathcal{P}_4 : \{0.9, 0.9, 0.95, 1\}$

The first two configurations of $\mathcal{P}$ test the fidelity of the model response when confronted with a singular secondary infection event some 30 days after the initial infection. The first configuration represents a normal response and is intended to calibrate the model for near optimal conditions. For $\mathcal{P}_1$, we would expect to see CTL production levels broadly characterised by low, elongated peak for primary infection, followed by an increase in memory CTL. Another expected observation

[2] in that $P(X_r|e) = 1$

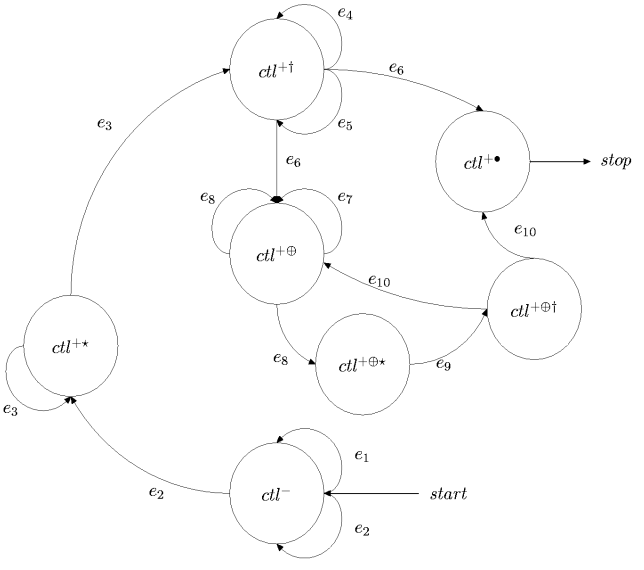


**Fig. 1.** A seven-state non-deterministic finite automata of the cytotoxic lymphocyte cell lifecycle. Transition events ($e_n$), which carry the same label, are *non-deterministic*.

is APC clearance: over some $6-10$ days for primary response, and significantly faster during secondary response. The second configuration is an increase in $\psi_3$ from 0.9 to 0.95 and is intended to test the impact of a 5% decline in the number of cells which transition to the effector memory state ($ctl^{+\dagger} \rightarrow ctl^{+\oplus}$). Some viral infections are known to case damage or loss of the memory pool [16], and we test to see the impact this has on our model. We test repeated reinfection with normal and depleted memory cell production ($\mathcal{P}_3$ and $\mathcal{P}_4$, respectively). Many pathogens are known to lead to acute and persistent viral infections, and we test the importance of memory cell production in these cases. Again we deplete the memory production by 5% and study the consequences of this loss. Section 4.1 examines the results of persistent infection in our model.

## 4 Results

The model is initially executed with parameter set $\mathcal{P}_1$ and $\mathcal{P}_2$ (with no repeat reinfection), and the results are shown in Fig. 2. In (a), the initial infection is visible at $\tau = 0$ with pathogen density $p_d = 5000$, (the broken line) and consequent effector response reaching a maximum value at $\tau = 300$, with $e_d = 8.2 \times 10^3$. Fig. 2(b) shows the antigen presenting cell population level (only). No memory cells are present during primary response, and as such, the effector cell population is made up entirely of clones produced by stimulated precursor cells. To the right of each effector cell peak is a plateau of memory cells. The slope of the CTL density peak is extreme, indicating that the state transitions

**Table 1.** Notation and definition of model entity states

| Notation | Definition |
|---|---|
| $ctl^{-}$ | naive recirculating effector precursor |
| $ctl^{+\star}$ | proliferating lymphocyte |
| $ctl^{+\bullet}$ | dead activated lymphocyte (apoptosis) |
| $ctl^{+\oplus}$ | activated memory effector |
| $ctl^{+\oplus\star}$ | activated proliferating memory effector |
| $ctl^{+\oplus\dagger}$ | activated memory effector |
| $ctl^{+\dagger}$ | armed activated effector |
| $apc^{+}$ | active infected antigen presenting cell |
| $apc^{+\bullet}$ | dead infected antigen presenting cell |

from $ctl^{+\star}$ to $ctl^{+\dagger}$ to $ctl^{+\oplus}$ (or $ctl^{+\bullet}$) occurring with a high degree of certainty. At time $\tau = 1500$ (day 31), secondary exposure to the same pathogen occurs, and the model exhibits following general behaviour: (i) the secondary immune response is preceeded by a pool of committed CTL memory cells which have already been primed to respond to the re-appearing pathogen, (ii) the activated CTL density is some 10 times higher than primary response, and does not last as long, and (iii) the pathogen is reduced to half its original level much more rapidly than during primary response. With $\mathcal{P}_1$, the model exhibits efficient detection and clearance behaviour associated with a healthy immune system. From Fig. 2, it can be seen the advantage in both time and infected cell clearance which is conferred on a response based largely on memory: the half life of the virus during primary response is around 3.25 days, with 90% pathogen clearance achieved at around $\tau = 480$, or 10 days of simulation time. Compared to secondary response on reinfection we see an infected cell half life of $\tau \approx 60$ or 1.25 days - an efficiency of around 87%. Effectively, this is because memory cells, having already been primed by a previous encounter with the specific pathogen, undergo expansion with lower death rates than during primary response: they therefore accumulate more quickly [17]. The results for $\mathcal{P}_2$ are shown in Fig. 2(c) and (d). Here, the probability of entering apoptosis is increased from 0.9 to 0.95. This means that the memory cell population would be around 5% of that activated effector population post-primary response. Recent work (notably [17]) has shown that some $\approx$ 90% of activated effector undergo apoptosis after primary response. Therefore, $\psi_3 = 0.95$ would represent an unusually high suppression of memory function. Clearly, the reduction of memory effector production should not effect primary response, and this is borne out by CTL density levels prior to $\tau = 1500$ (c). We see a normal 10-day clearance regime (d) during primary response, but a less effective response during reinfection: in fact, the memory cell pool in the time range $500 \leq \tau \leq 1500$ has fallen to $\approx 500$. Once reinfection occurs, the APC

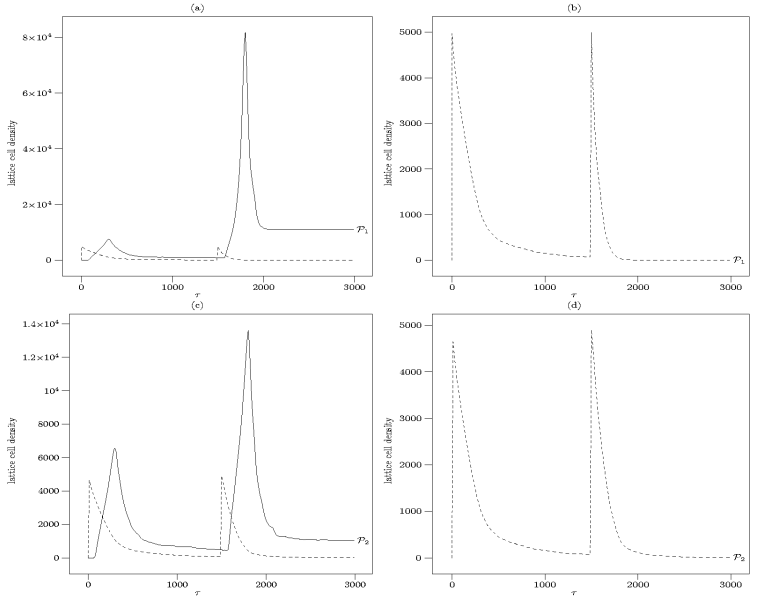


**Fig. 2.** CTL and pathogen lattice density levels (a),(c) over a simulated 62.5 day period, with an initial infection at time $\tau = 0$ and a reinfection by the same pathogen occurring at $\tau = 1500$, for 3 values of $\mathcal{P}$. Antigen presenting cell (APC) density is shown by the broken line, with the solid line indicating levels of effector memory and activated cells combined. For clarity, (b),(d) show population levels for APC for each $\mathcal{P}$.

population is cleared some 31% more effectively than during primary response. The APC half life is $\tau = 108$, 90% clearance is achieved after reinfection at $\tau \approx 1788$ (or some 5.9 days of simulated time). However, the characteristics of $\mathcal{P}_2$ are significantly degraded compared to that observed in $\mathcal{P}_1$.

### 4.1 Persistent Reinfection

Some viral pathogens are capable of persistent reinfection, in that, although population levels of infected antigen presenting cells may decline in response to clearance pressure by a specific CTL response, over time, the number of infected cells rises to chronic and sometimes acute levels. Examples of such viruses are HIV, HTLV, hepatitis C (HCV), hepatitis B virus, CMV EBV and rubella [16]. Such persistent reinfection pathogens have been associated with normal immune function suppression. In this section, we simulate persistent reinfection by randomly scattering a repeat 'dose' of the pathogen, introduced at $\tau + 300n, n = 0, 1, ..., 9$. This reinfection pattern is a represents a resurgence of infected cells every 6.25 days, in discrete bursts. The results of this simulation are shown in Fig. 3.

With respect to Fig. 3 (a), the response to the first reinfection is clearly strong: some $3.8 \times 10^5$ lymphocytes are generated and the reinfection is rapidly

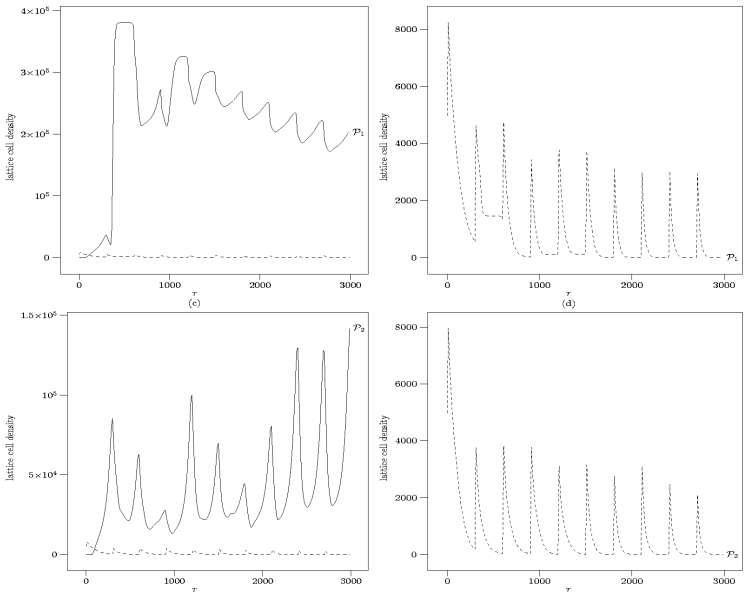


**Fig. 3.** The model is exposed to repeated infection events, arising at time $\tau = 300n, n = 0, 1, ..., 9$, equivalent to an infection every 6 days.

eliminated. As further infections arise starting at $\tau = 600$, the existing memory pool never falls below $1.8 \times 10^5$, and is critical in bringing the repeated reinfections under control in time periods (b) which rarely exceed 130 timesteps (or 2.8 days of simulated time). We also see from (a) that slightly lower responses are sufficient in order to effect optimal clearance. Results from (a) and (b) support the clinical findings that the memory cell levels tends to be higher after secondary and tertiary infections [17], which in turn, supports the clinical practice of vaccination boosting. Finally, when the simulation is executed with diminished memory cell creation and repeatedly stressed with reinfection ($\mathcal{P}_4$), average primary and secondary response levels are similar (around $1.2 \times 10^4$). Each response is characterised by rapid expansion and reduction of effector lymphocyte clones. There are no memory cells to confer clearance advantage, and each response is initiated from low levels (around $1.2 \times 10^2$).

## 5 Discussion and Conclusions

The approach taken in this research was to construct a stochastic model of the effector T cell lifecycle, in order to study a distribution of possible simulation outcomes. We have shown how the model reproduces well the time and space dynamics of initial and secondary infection. In addition, we believe the research is valuable in modelling the relationship between repeated reinfection and effector

cell transition to memory or apoptosis. We have demonstrated how repeated reinfection can be controlled only within a limited range of $\psi_3$: too much memory causes the lymphatic compartment to fill-up, too little memory induces the need for clonal expansion from naive precursor cells, and a elongated APC clearance profile. When the ratio of apoptosis to memory is 'just right' ($0.88 \leq \psi_3 \leq 0.92$), antigen presenting cell levels (during repeated reinfection) are brought under control in increasingly rapid time frames. The next steps in this research are to test the homeostasis of our model: where does the model break down, and what insight does this provide. Very recent clinical work [16] suggests that the immune system must periodically preferentially eliminate some memory cells which exhibit poor cross-reactivity. One of the benefits of the the stochastic effector T cell lifecycle model presented here is the relative ease with which this theory could be investigated. The benefits of selective memory cells reduction may form the basis of further work with this model.

## References

1. Wolfram, S.: Cellular Automata as Simple Self-Organizing Systems. Nature **1** (1982) 1
2. Wolfram, S.: A New Kind of Science. Wolfram Media (2001)
3. Stauffer, D., Pandey, R.B.: Immunologically motivated simulation of cellular automata. Computers in Physics **6** (1992) 404
4. Castiglione, F., Bernaschi, M., Succi, S.: Simulating the Immune Response on a Distributed Parallel Computer. Int. J. Mod. Phys. **8** (1997) 527
5. Mannion, R., Ruskin, H., Pandey, R.: Effect of Mutation on Helper T-cells and Viral Population: A Computer Simulation Model for HIV. Theor. in Biosci. **199(2)** (2000) 145–155
6. dos Santos, R.M.Z., Coutinho, S.: Dynamics of HIV Infection: A Cellular Automata Approach. Phys. Rev. Lett. **87** (2001) 168102
7. Bernaschi, M., Castiglione, F.: Design and implementation of an immune system simulator. Computers in Biology and Medicine **31** (2001) 303–331
8. Burns, J., Ruskin, H.J.: Network Topology in Immune System Shape Space. In Sloot, P., Gorbachev, Y., eds.: Computational Science - ICCS 2004. Volume 3038 of Lecture Notes in Computer Science., Berlin Heidelberg, Springer-Verlag (2004) 1094–1101
9. Germain, R.N.: The Art of the Probable: System Control in the Adaptive Immune System. Science **293** (2001) 240–245
10. Perelson, A.S., Oster, G.F.: Theoretical Studies of Clonal Selection: Minimal Antibody Repertoire Size and Reliability of Self-Non-Self Discrimination. J.Theor. Biol. **81(4)** (1979) 645–70
11. Burns, J., Ruskin, H.J.: Diversity Emergence and Dynamics During Primary Immune Response: A Shape Space, Physical Space Model. Theor. in Biosci. **123(2)** (2004) 183–194
12. Hopcroft, J.E., Ullman, J.D.: Introduction to Automata Theory, Languages and Computation. Addison Wesley (1979)
13. Murali-Krishna, K., Lau, L.L., Sambhara, S., Lemonnier, F., Altman, J., Ahmed, R.: Persistence of Memory CD8 T Cells in MHC Class I-Deficient Mice. J. Exp. Med. **286** (1999) 1377–1381

14. De Boer, R.J., Oprea, M., Kaja, R.A., Murali-Krishna, Ahmed, R., Perelson, A.S.: Recruitment Times, Proliferation, and Apoptosis Rates during the $CD8^+$ T-Cell Response to Lymphocytic Choriomeningitis Virus. J. Virol. **75(22)** (2001) 10663–10669
15. Badovinac, V.P., Porter, B.B., Harty, J.T.: CD8+ T cell contraction is controlled by early inflammation. Nat. Immunol. **5** (2004) 809–817
16. Kim, S., Walsh, R.: Comprehensive early and lasting loss of memory CD8 T cells and functional memory during acute and persistent viral infections. J. Immunol. **172(5)** (2004) 3139–3150
17. Grayson, J., Harrington, L., Lanier, J., Wherry, E., Ahmed, R.: Differential Sensitivity of Naive and Memory CD8+ T cells to Apoptosis in Vivo. J. Immunol. **169(7)** (2002) 3760–3770